Exceptional-point dynamics in photonic honeycomb lattices with $\mathcal{PT}$ symmetry

Hamidreza Ramezani,[1] Tsampikos Kottos,[1,2] Vassilios Kovanis,[3] and Demetrios N. Christodoulides[4]
[1]*Department of Physics, Wesleyan University, Middletown, Connecticut 06459, USA*
[2]*MPI for Dynamics and Self-Organization, Bunsenstraße 10, D-37073 Göttingen, Germany*
[3]*Air Force Research Laboratory, Sensors Directorate, Wright Patterson Air Force Base, Ohio 45433, USA*
[4]*College of Optics & Photonics-CREOL, University of Central Florida, Orlando, Florida 32816, USA*
(Received 3 August 2011; revised manuscript received 2 December 2011; published 17 January 2012)

We theoretically investigate the flow of electromagnetic waves in complex honeycomb photonic lattices with local $\mathcal{PT}$ symmetries. Such $\mathcal{PT}$ structure is introduced via a judicious arrangement of gain and loss across the honeycomb lattice, characterized by a gain and loss parameter γ. We found a class of conical diffraction phenomena where the formed cone is brighter and travels along the lattice with a transverse speed proportional to $\sqrt{\gamma}$.

DOI: 10.1103/PhysRevA.85.013818 PACS number(s): 42.25.Bs, 11.30.Er, 42.70.Qs

I. INTRODUCTION

Conical refraction phenomena, i.e., the spreading into a hollow cone of an unpolarized light beam entering a biaxial crystal along its optic axis, are fundamental in classical optics and in mathematical physics [1–4]. Originally predicted by Hamilton in 1837 [3] and experimentally observed by Lloyd [4], these phenomena have been intensively studied in recent years by a large community of theorists and experimentalists [1–8]. The physical origin of the phenomenon is associated with the existence of the legendary *diabolical points*, which emerge along the axis of intersection of the two shells associated with the wave surface. Around a diabolical point the energy dispersion relation is linear while the direction of the group velocity is not uniquely defined. Recently, conical diffraction was observed in two-dimensional photonic honeycomb lattices [5] which share key common features, including the existence of diabolical points, with the band structure of graphene in condensed matter physics literature. In graphene, the electrons around the diabolical points of the band structure behave as *massless relativistic fermions*, thus resulting in extremely high electron mobility. Both photonic and electronic graphene structures allow us to test experimentally various legendary predictions of relativistic quantum mechanics such as the Klein paradox [9] and the dynamics of optical tachyons [10].

While diabolical points are spectral singularities associated with Hermitian systems, for pseudo-Hermitian Hamiltonians, like those used for the theoretical description of non-Hermitian optics, a topologically different singularity may appear: an *exceptional point* (EP), where not only the eigenvalues but also the associated eigenstates coalesce. Pseudo-Hermitian optics is a rapidly developing field which aims, via a judicious design that involves the combination of delicately balanced amplification and absorption regions together with the modulation of the index of refraction, to achieve new classes of synthetic metamaterials that can give rise to altogether new physical behavior and novel functionality [11,12]. The idea can be carried out via index-guided geometries with special antilinear symmetries. Adopting a Schrödinger language that is applicable in the paraxial approximation, the effective Hamiltonian that governs the optical beam evolution is non-Hermitian and commutes with the combined parity ($\mathcal{P}$) and time ($\mathcal{T}$) operator [13–15]. In optics, $\mathcal{PT}$ symmetry demands that the complex refractive index obeys the condition $n(\mathbf{r}) = n^*(-\mathbf{r})$. It can be shown that for such structures, a real propagation constant (eigenenergies in the Hamiltonian language) exists for some range (the so-called exact phase) of the gain and loss coefficient. For larger values of this coefficient, the system undergoes a *spontaneous symmetry breaking*, corresponding to a transition from real to complex spectra (the so-called broken phase). The phase transition point shows all the characteristics of an exceptional-point singularity.

$\mathcal{PT}$ symmetries are not only novel mathematical curiosities. In a series of recent experimental papers, $\mathcal{PT}$ dynamics were investigated and key predictions confirmed and demonstrated [16–19]. Symmetry breaking has been experimentally observed in non-Hermitian structures [16–18], while power-law growth—characteristic of phase transitions—of the total energy has been demonstrated close to the exceptional points in Ref. [18]. In a silicon platform claims have been made that nonreciprocal light propagation in a silicon photonic circuit has been recorded [19]. $\mathcal{PT}$-synthetic materials can exhibit several intriguing features. These include, among others, power oscillations and nonreciprocity of light propagation [11,16,20,21], nonreciprocal Bloch oscillations [22], and unidirectional invisibility [23]. More specifically, a recent paper has proposed photonic honeycomb lattices with $\mathcal{PT}$ symmetry [10]. Interestingly, that work has shown that introducing alternating gain and loss to a honeycomb system prohibits $\mathcal{PT}$ symmetry, but adding appropriate strain (direction and strength) restores the symmetry, giving rise to $\mathcal{PT}$-symmetric photonic lattices [10]. Moreover, the mentioned work has found that in such systems, much higher group velocities can be achieved (compared with non-$\mathcal{PT}$-symmetry breaking systems), corresponding to a tachyonic dispersion relation [10]. In the nonlinear domain, such pseudo-Hermitian nonreciprocal effects can be used to realize a new generation of on-chip isolators and circulators [24]. Other results within the framework of $\mathcal{PT}$ optics include the realization of coherent perfect laser absorber [25], spatial optical switches [26], and nonlinear switching structures [27]. Despite the wealth of results on transport properties of $\mathcal{PT}$-symmetric one-dimensional optical structures, the properties of high-dimensional $\mathcal{PT}$ optical lattices (with the exception of few recent studies [11,28]) has remained so far essentially unexplored.

Report Documentation Page

Form Approved
OMB No. 0704-0188

1. REPORT DATE	2. REPORT TYPE	3. DATES COVERED
17 JAN 2012		**00-00-2012 to 00-00-2012**

4. TITLE AND SUBTITLE	5a. CONTRACT NUMBER
Exceptional-point dynamics in photonic honeycomb lattices with PT symmetry	5b. GRANT NUMBER
	5c. PROGRAM ELEMENT NUMBER
6. AUTHOR(S)	5d. PROJECT NUMBER
	5e. TASK NUMBER
	5f. WORK UNIT NUMBER
7. PERFORMING ORGANIZATION NAME(S) AND ADDRESS(ES) **University of Central Florida,CREOL, College of Optics and Photonics,4000 Central Florida Blvd,Orlando,FL,32816**	8. PERFORMING ORGANIZATION REPORT NUMBER
9. SPONSORING/MONITORING AGENCY NAME(S) AND ADDRESS(ES)	10. SPONSOR/MONITOR'S ACRONYM(S)
	11. SPONSOR/MONITOR'S REPORT NUMBER(S)

12. DISTRIBUTION/AVAILABILITY STATEMENT
Approved for public release; distribution unlimited

13. SUPPLEMENTARY NOTES

14. ABSTRACT

15. SUBJECT TERMS

16. SECURITY CLASSIFICATION OF:			17. LIMITATION OF ABSTRACT	18. NUMBER OF PAGES	19a. NAME OF RESPONSIBLE PERSON
a. REPORT **unclassified**	b. ABSTRACT **unclassified**	c. THIS PAGE **unclassified**	**Same as Report (SAR)**	**6**	

Recently, it was pointed out [29] that $\mathcal{PT}$-symmetric Hamiltonians are a special case of pseudo-Hermitian Hamiltonians, i.e., Hamiltonians that have an *antilinear* symmetry [30–32]. Such Hamiltonians commute with an antilinear operator $\mathcal{ST}$, where $\mathcal{S}$ is a generic linear operator. The corresponding Hamiltonian $\mathcal{H}$ is termed *generalized* $\mathcal{PT}$ symmetric. In a similar manner as in the case of $\mathcal{PT}$ symmetry, one finds that if the eigenstates of $\mathcal{H}$ are also eigenstates of the $\mathcal{ST}$ operator then all the eigenvalues of $\mathcal{H}$ are strictly real and the $\mathcal{ST}$ symmetry is said to be *exact*. Otherwise the symmetry is said to be *broken*. An example case of a generalized $\mathcal{PT}$-symmetric optical structure is the one reported in [33] (see also [20]). The unifying feature of these systems is that they are built of a particular kind of "building block" which below is referred to as a *dimer*. Each dimer in itself does have $\mathcal{PT}$ symmetry and it can be represented as a pair of sites with assigned energies ϵ_n, ϵ_n^*. The system is composed of such dimers, coupled in some way. For an arbitrary choice of the site energies ϵ_n and coupling between the dimers, the system as a whole does not possess $\mathcal{PT}$ symmetry (indeed, such *global* $\mathcal{PT}$ symmetry would require precise relation between various ϵ_n and coupling symmetry between the dimers). On the other hand, since each dimer is $\mathcal{PT}$ symmetric, with respect to its own center, there is some kind of "local" $\mathcal{PT}$ symmetry (which we shall define as $\mathcal{P}_d\mathcal{T}$ symmetry). The main message of these papers is that, $\mathcal{P}_d\mathcal{T}$ symmetry ensures a robust region of parameters in which the system has an entirely real spectrum. Below, we will use the term $\mathcal{PT}$ symmetry in a loose manner and we will include also systems with generalized $\mathcal{PT}$ symmetry.

In this paper we investigate beam propagation in non-Hermitian two-dimensional photonic honeycomb lattices with $\mathcal{PT}$ symmetry and probe for the possibility of abnormal diffraction. We find a type of conical diffraction that is associated with the spontaneously $\mathcal{PT}$-symmetry-breaking phase transition point. Despite the fact that at the EP the Hilbert space collapses, the emerging cone is brighter and propagates with a transverse velocity that is controlled by the gain and loss parameter γ.

The organization of the paper is as follows: In Sec. II, we present the mathematical model. In Sec. III we analyze the stationary properties of the system and introduce a criterion based on the degree of nonorthogonality of the eigenmodes in order to identify the EP for finite system sizes. The beam dynamics is studied in Sec. IV. First, we study numerically the beam evolution in Sec. IV A, while the theoretical analysis is performed in Sec. IV B. Our conclusions are given in Sec. V.

II. PHOTONIC LATTICE MODEL

We consider a two-dimensional honeycomb photonic lattice of coupled optical waveguides. Each waveguide supports only one mode, while light is transferred from waveguide to waveguide through optical tunneling. A schematic of the setup is shown in Fig. 1. The lattice consist of two types of waveguides: type A is made from lossy material (green), whereas type B exhibits an equal amount of gain (red). Their arrangement in space is such that they form coupled A-B dimers with inter- and intradimer couplings t_a and t, respectively. Such structure, apart from a global $\mathcal{PT}$ symmetry,

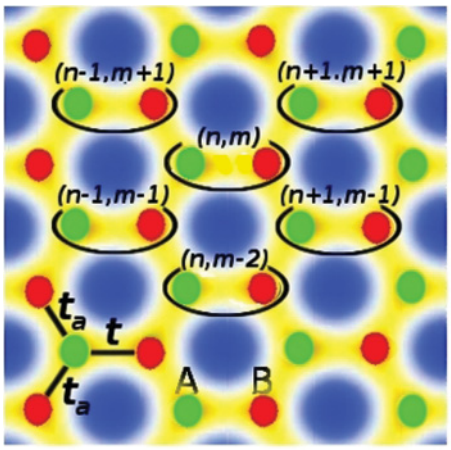

FIG. 1. (Color online) Honeycomb photonic lattice structure with intradimer coupling t and interdimer coupling $t_a = 1$. Sublattice (lossy waveguide) $a_{n,m}$ is shown by green (gray in the black-and-white printed version) circles while sublattice (gain waveguide) $b_{n,m}$ is shown by the red (dark in the black-and-white printed version) circles. Each dimer is distinguished by index n and m. The field is coupled evanescently between the waveguides.

respects also another antilinear symmetry (in Ref. [33] we coined this $\mathcal{P}_d\mathcal{T}$ symmetry) which is related to the local $\mathcal{PT}$ symmetry of each individual dimer.

Without loss of generality we rescale everything in units of the interdimer coupling $t_a = 1$. In the tight binding description, the diffraction dynamics of the mode electric field amplitude $\Psi_{n,m} = (a_{n,m}, b_{n,m})^T$ at the (n,m)th dimer evolves according to the following Schrödinger-like equation:

$$\begin{aligned} i\frac{da_{n,m}}{dz} + \epsilon a_{n,m} + b_{n-1,m+1} + b_{n-1,m-1} + t b_{n,m} = 0, \\ i\frac{db_{n,m}}{dz} + \epsilon^* b_{n,m} + a_{n+1,m+1} + a_{n+1,m-1} + t a_{n,m} = 0, \end{aligned} \tag{1}$$

where $\epsilon = \epsilon_0 + i\gamma$ is related to the refractive index [11]. Without loss of generality, we assume $\epsilon_0 = 0$ and $\gamma > 0$.

It is useful to work in the momentum space. To this end, we write the field amplitudes $\Psi_{n,m}$ in their Fourier representation, i.e.,

$$\begin{aligned} a_{n,m}(z) = \frac{1}{(2\pi)^2}\int_{-\pi}^{\pi} dk_x dk_y \tilde{a}_{k_x,k_y}(z)\exp(i[nk_x + mk_y]), \\ b_{n,m}(z) = \frac{1}{(2\pi)^2}\int_{-\pi}^{\pi} dk_x dk_y \tilde{b}_{k_x,k_y}(z)\exp(i[nk_x + mk_y]). \end{aligned} \tag{2}$$

Substitution of Eq. (2) into Eq. (1) leads to the following set of coupled differential equations in the momentum space:

$$i\frac{d}{dz}\begin{pmatrix}\tilde{a}_{\mathbf{k}}(z)\\ \tilde{b}_{\mathbf{k}}(z)\end{pmatrix} = H_{\mathbf{k}}\begin{pmatrix}\tilde{a}_{\mathbf{k}}(z)\\ \tilde{b}_{\mathbf{k}}(z)\end{pmatrix}, \tag{3}$$

where

$$H_{\mathbf{k}} = \begin{pmatrix}-i\gamma & D(\mathbf{k})\\ D(\mathbf{k})^* & i\gamma\end{pmatrix}. \tag{4}$$

and

$$D(\mathbf{k}) = -(t + 2e^{-ik_x}\cos k_y); \quad \mathbf{k} \equiv (k_x, k_y). \tag{5}$$

In other words, because of the translational invariance of the system, the equations of motion in the Fourier representation break up into 2×2 blocks, one for each value of momentum $\mathbf{k}$. The two-component wave functions for different $\mathbf{k}$ values are then decoupled, thus allowing a simple theoretical description of the system.

III. EIGENMODES ANALYSIS

We start our analysis with the study of the stationary solutions corresponding to Eq. (3). Substituting the stationary form

$$(\tilde{a}_{n,m},\tilde{b}_{n,m})^T = \exp(-i\mathcal{E}z)(A,B)^T \tag{6}$$

in Eq. (3), we get

$$\mathcal{E}\begin{pmatrix} A \\ B \end{pmatrix} = H_{\mathbf{k}}\begin{pmatrix} A \\ B \end{pmatrix}. \tag{7}$$

The spectrum is obtained by requesting a nontrivial solution, i.e., $(A,B) \neq 0$. The corresponding dispersion relation [10] has the form

$$\mathcal{E}_{\pm} = \pm\sqrt{|D(\mathbf{k})|^2 - \gamma^2}. \tag{8}$$

For $\gamma = 0$ the dispersion relation is

$$\mathcal{E} = \pm|D(\mathbf{k})|, \tag{9}$$

and we have two bands of width $t+2$. There are three pairs of diabolic points (DPs):

$$\begin{aligned} \mathbf{k}_0^{\pm,\mp} &= \left(\pm\pi, \pm\arccos\frac{t}{2}\right), \\ \mathbf{k}_1^{\pm} &= \left[0, \pm\left(\pi - \arccos\frac{t}{2}\right)\right]. \end{aligned} \tag{10}$$

Expansion of $D(\mathbf{k})$ up to the first order around the DPs leads to

$$D(\mathbf{k}) \approx it\eta_x \mp \sqrt{4-t^2}\eta_y. \tag{11}$$

Substituting the above expression in the energy dispersion given by Eq. (8), we get the linear relation

$$\mathcal{E}_{\mathbf{k}} \approx \pm\left[t^2\eta_x^2 + (4-t^2)\eta_y^2\right]^{1/2}, \tag{12}$$

where $\eta_{x,y} = k_{x,y} - (k_{0,1})_{x,y}$.

The standard passive ($\gamma = 0$) honeycomb lattice (zero strain) corresponds to $t = 1$. In this case, there are three pairs of DPs at [see Fig. 2(a)]

$$\begin{aligned} \mathbf{k}_0^{\pm,\mp} &= \left(\pm\pi, \pm\frac{\pi}{3}\right), \\ \mathbf{k}_1^{\pm} &= \left(0, \pm\frac{2\pi}{3}\right). \end{aligned} \tag{13}$$

For $1 < t < 2$ the two pairs of DPs at $\mathbf{k}_0^{\pm,\mp}$ start moving toward each other while the pair at $\mathbf{k}_1^{\pm}$ moves away from one another. At $t = 2$ a *degeneracy* occurs, i.e., $\mathbf{k}_0^{\pm,\mp} = (\pm\pi,0)$. At the same time the dispersion relation $\mathcal{E}$ around $\mathbf{k}_0^{\pm,\mp}$ and $\mathbf{k}_1^{\pm}$ is linear only in the k_x direction (and quadratic in the k_y). For $t > 2$ the two energy surfaces move away from each other and a gap between them is created [see Fig. 2(b)]. Therefore for $t \geqslant 2$ the DPs disappear for $\gamma = 0$, and the conical diffraction is destroyed [6,34].

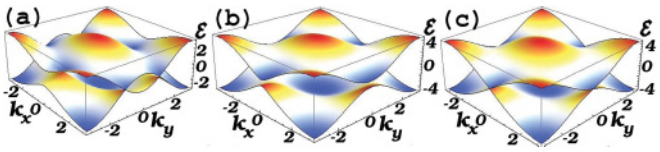

FIG. 2. (Color online) Energy surfaces for a honeycomb lattice with $t_a = 1$ and (a) $(t,\gamma) = (1,0)$ where a DP is present, (b) $(t,\gamma) = (2.5,0)$ where a band gap has been created, and (c) $(t,\gamma) = (2.5,0.5)$ where a gain and loss parameter led to the creation of a EP.

By introducing gain and loss to the system described by Eq. (1), the resulting effective Hamiltonian which describes the paraxial evolution becomes non-Hermitian. In fact, for $1 \leqslant t \leqslant 2$, any value of γ results in complex eigenvalues, i.e., the system is in the broken $\mathcal{PT}$-symmetry phase. The resulting dispersion relation resembles the dispersion relation of relativistic particles with imaginary mass, as was recently discussed in Ref. [10].

In the case of $t > 2$ the size of the gap between the two bands can be controlled by manipulating the gain and loss parameter γ. In this case, there is a γ domain, corresponding to the exact phase, for which the energies are real. It turns out from Eq. (8) that the line

$$\gamma_{\mathcal{PT}} = t - 2 \tag{14}$$

defines the phase transition from exact to broken $\mathcal{PT}$ symmetry [10]. The mechanism for this symmetry breaking is the crossing between levels, associated with the exceptional points

$$\begin{aligned} &\mathbf{k}_{\mathrm{EP}}^{\pm} = (0, \pm\pi) \\ &\quad\text{or} \\ &\mathbf{k}_{\mathrm{EP}}^{\pm} = (\pm\pi,0) \end{aligned} \tag{15}$$

[see Fig. 2(c)] and belonging to different bands [33]: it follows from Eq. (8), that when $\gamma = \gamma_{\mathcal{PT}}$, the gap disappears and the two (real) levels at the "inner" band edges become degenerate. Evaluation of $D(k_x,k_y)$ to second order in (η_x,η_y) around the degeneracy points leads to

$$D(\eta_x,\eta_y) \approx -(\gamma_{\mathcal{PT}} + 2i\eta_x + \eta^2), \quad \eta^2 \equiv \eta_x^2 + \eta_y^2, \tag{16}$$

thus resulting in the dispersion relation

$$\mathcal{E} = \pm\sqrt{2\gamma_{\mathcal{PT}}\eta_y^2 + (2\gamma_{\mathcal{PT}} + 4)\eta_x^2}. \tag{17}$$

For large $\gamma_{\mathcal{PT}}$ values (i.e., $\gamma_{\mathcal{PT}} \gg 2$) one can approximate the above equation to get

$$\mathcal{E} \approx \pm\sqrt{2\gamma_{\mathcal{PT}}}\eta. \tag{18}$$

This comment will become important in the analysis of optical beam propagation discussed in Sec. IV.

Next, we turn to the analysis and characterization of the biorthogonal set of eigenvectors of our non-Hermitian system. The target here is to identify the proximity to the exceptional point in the case of finite Hilbert spaces, where finite-size effects might play an important role in the analysis of the dynamics. The latter do not respect the standard (Euclidian) orthonormalization condition. Let $\langle L_n|$ and $|R_n\rangle$ denote the left and right eigenvectors of the non-Hermitian Hamiltonian

$\mathcal{H}$ corresponding to the eigenvalue $\mathcal{E}_n$, i.e.,

$$\langle L_n|\mathcal{H} = \langle L_n|\mathcal{E}_n, \qquad \mathcal{H}|R_n\rangle = \mathcal{E}_n|R_n\rangle. \tag{19}$$

The vectors can be normalized to satisfy

$$\langle L_n|R_m\rangle = \delta_{nm}, \tag{20}$$

while

$$\sum_{n}^{\mathcal{N}} |R_n\rangle\langle L_n| = 1. \tag{21}$$

Above, $\mathcal{N}$ is the dimension of the Hilbert space.

An observable that measures the nonorthogonality of the modes and can be used to identify the proximity to the EP in the presence of finite-size effects is the so-called Petermann factor, which is defined as [35]

$$K_{nm} = \langle L_n|L_m\rangle\langle R_m|R_n\rangle. \tag{22}$$

We have studied the mean (diagonal) Petermann factor

$$\overline{K} = \frac{1}{\mathcal{N}}\sum_{n=1}^{\mathcal{N}} K_{nn}, \tag{23}$$

which takes the value of unity if the eigenfunctions of the system are orthogonal, while it is larger than unity in the opposite case. At the EP, a pair of eigenvectors associated with the corresponding degenerate eigenvalues coalesce, leading to a *collapse* of the Hilbert space. At this point, the Petermann factor diverges as [20,36]

$$\overline{K} \sim 1/|\gamma - \gamma_{\mathcal{PT}}|. \tag{24}$$

. This indicates strong correlations between the spectrum and the eigenvectors, which can affect drastically the dynamics, as we will see later.

In Fig. 3 we present our calculations for $\overline{K}$ for different (t,γ) values and various system sizes. We find that as $\mathcal{N}$ increases, the divergence approaches the line $\gamma_{\mathcal{PT}} = t - 2$, which was derived previously [see Eq. (14)] for the case of infinite graphene.

IV. DYNAMICS

Armed with the previous knowledge about the eigenmode properties of the $\mathcal{PT}$-symmetric graphene, we are now ready to study beam propagation in $\mathcal{PT}$-symmetric honeycomb lattices at the vicinity of the EPs. The question at hand is whether the collapse of the Hilbert space at the EP will affect the conical diffraction (CD) pattern, and if yes, what is the emerging dynamical picture.

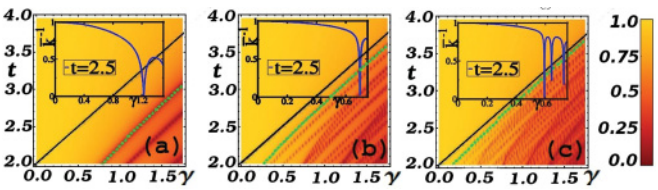

FIG. 3. (Color online) Inverse Petermann factor for various system sizes (a) $\mathcal{N} = 24$, (b) $\mathcal{N} = 168$, and (c) $\mathcal{N} = 440$. The asymptotic line $\gamma_{\mathcal{PT}} = t - 2$ (black solid line) is approached by our numerical data (zero of $\overline{K}^{-1}$) for increasing $\mathcal{N}$. The green dotted line is plotted to guide the eye. The insets show representative $\overline{K}^{-1}$'s vs γ for a fixed coupling $t = 2.5$.

A. Numerical analysis

We first study wave propagation in the honeycomb lattice numerically (Fig. 4), by launching a beam with the structure of a Bloch mode associated with the EP, multiplied by a Gaussian envelope. The Bloch modes at the tip can be constructed from pairs of plane waves with $\mathbf{k}$ vectors of opposite pairs of exceptional points. Thus, interfering two plane waves at angles associated with opposite EP yields the phase structure of the modes from these points. Multiplying these waves by an envelope yields a superposition of Bloch modes in a region around these points. Figure 4 shows an example of the propagation of a beam constructed to excite a Gaussian superposition of Bloch modes around an EP. The input beam has a bell-shape structure, which, after some distance, transforms into the ring-like characteristic of conical diffraction [34]. From there on, the ring is propagating in the lattice by keeping its width constant while its radius is increasing linearly with distance. The invariance of the ring thickness and structure manifests a (quasi-) linear dispersion relation above and below the EP (see Fig. 2); hence, the diffraction coefficient for wave packets constructed from Bloch modes in that region is zero (infinite effective mass). This is especially interesting because the ring itself is a manifestation of the dispersion properties at the EP itself, where the diffraction coefficient is infinite (zero-effective mass). As a result, the ring forms a light cone in the lattice. The appearance of CD in the case of $\mathcal{PT}$ lattices where the eigenvectors are nonorthogonal and coalesce at the EP singularity provides a clear indication that the phenomenon is insensitive to the eigenmodes structure and that it depends only on the properties of the dispersion relation.

The $\mathcal{PT}$-symmetric conical diffraction shows some unique characteristics with respect to the CD found in the case of beam propagation around DPs for passive honeycomb lattices

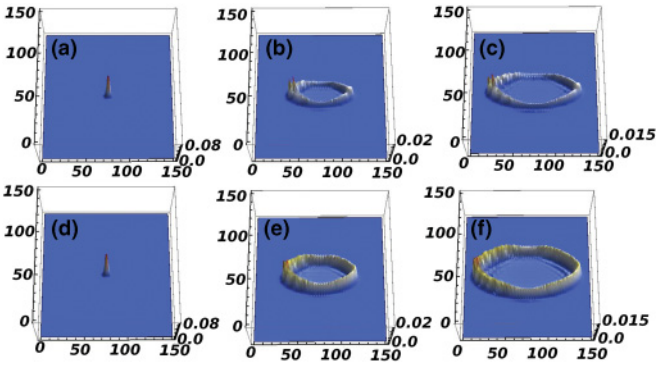

FIG. 4. (Color online) Propagation of a Gaussian superposition of Bloch modes associated with the vicinity of a EP at $\mathbf{k} = (0, \pm\pi)$, in a $\mathcal{PT}$-symmetric honeycomb lattice. Shown is the beam intensity at normalized propagation distances of (a),(d) $z = 0$; (b),(e)$z = 10$; (c),(f) $z = 15$, for $\gamma_{\mathcal{PT}} = 1$ and $t = 3$ (upper panels) and $\gamma_{\mathcal{PT}} = 2$ and $t = 4$ (lower panels). The input bell-shaped beam transforms into a ring-like structure of light of a nonvarying thickness.

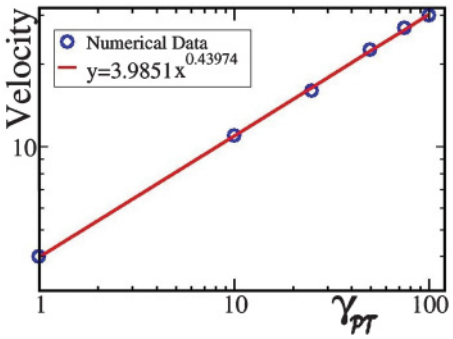

FIG. 5. (Color online) Transverse velocity of the spreading ring vs the $\gamma_{\mathcal{PT}}$. Numerical simulations approve theoretical predictions of the transverse speed of the CD, which is $v_g \propto \sqrt{\gamma_{\mathcal{PT}}}$.

(i.e., $\gamma = 0$). A profound difference is associated with the fact that now the transverse speed of the cone is increased [10], and in fact it can be controlled by the magnitude of the gain and loss parameter at the symmetry-breaking point $\gamma_{\mathcal{PT}}$. This is shown in Fig. 4 where we compare the spreading of a CD for two different $\gamma_{\mathcal{PT}}$ values.

In Fig. 5, we report in a double logarithmic plot, our numerical measurements for the transverse velocity of the spreading ring for various $\gamma_{\mathcal{PT}}$ values. The best linear fitting to the numerical data shows that transverse speed of the cone is proportional to $\sqrt{\gamma_{\mathcal{PT}}}$. This behavior can be understood qualitatively by realizing that the group velocity near the EPs is

$$v_g = \partial\mathcal{E}/\partial\mathbf{k} \sim \sqrt{2\gamma_{\mathcal{PT}}} \tag{25}$$

[see Eqs.(17) and (18)]. At the same time we find that the resulting $\mathcal{PT}$ cone is brighter with respect to the one found in passive lattices [5] (i.e., the field intensity of the conical wavefront is larger).

B. Theoretical considerations

It is possible to gain valuable insight into the features of $\mathcal{PT}$-conical diffraction by considering the field evolution in the momentum space. We consider for simplicity an initial distribution $[\tilde{a}_{\mathbf{k}}(0),\tilde{b}_{\mathbf{k}}(0)]^T$ that is symmetric around the EP while it decays exponentially away from it. Specifically we assume

$$[\tilde{a}_{\mathbf{k}}(0),\tilde{b}_{\mathbf{k}}(0)]^T = e^{-g\sqrt{\eta_x^2+\eta_y^2}}(1,0)^T. \tag{26}$$

Next, we calculate the evolution matrix $\mathbf{U} \equiv e^{-i\mathbf{H}_{\mathbf{k}}z}$ where $\mathbf{H}_{\mathbf{k}}$ is given by Eq. (4). After a straightforward algebra and using the fact that

$$\mathbf{H}_{\mathbf{k}}{}^2 = \mathcal{E}^2 \times \mathbf{1}, \tag{27}$$

where $\mathbf{1}$ is the unity matrix, we get

$$\mathbf{U} = \cos(z|\mathcal{E}|)\mathbf{1} - i[\sin(z|\mathcal{E}|)/|\mathcal{E}|]\mathbf{H}_{\mathbf{k}}. \tag{28}$$

Equation (28) is the starting point of our analysis. Substituting Eqs. (4), (16), and (17), we find that the evolving amplitude of the field $(a_{n,m},b_{n,m})$ is

$$\begin{aligned} a_{n,m}(z) &\approx \sum_{l=1,2} \frac{(-1)^l i[z - \gamma_{\mathcal{PT}}\phi(n,m,z,g)] + g}{\phi(n,m,z,g)^{3/2}}, \\ b_{n,m}(z) &\approx \sum_{l=1,2} \frac{(-1)^{l+1}\left[\gamma_{\mathcal{PT}}\phi(n,m,z,g) + \frac{n}{\sqrt{2\gamma_{\mathcal{PT}}+4}}\right]}{\phi(n,m,z,g)^{3/2}}, \end{aligned} \tag{29}$$

where

$$\begin{aligned} \phi(n,m,z,g) = [g + (-1)^l iz]^2 + n^2/(2\gamma_{\mathcal{PT}} + 4) \\ + m^2/(2\gamma_{\mathcal{PT}}). \end{aligned} \tag{30}$$

Although our simplified calculations are not able to capture all the features of the propagating cone, the above expression encompasses the main characteristics of the conical diffraction that we have observed in our numerical simulations. At $z = 0$, Eq. (29) resembles a Lorentzian, which slowly transforms into a ring of light, whose radius expands linearly with z with velocity $\sqrt{2\gamma_{\mathcal{PT}}}$, while its thickness remains unchanged. At the same time the field intensity on the ring in the case of $\mathcal{PT}$-symmetric lattices is brighter than the one corresponding to passive honeycomb lattices (i.e., $1/z^2$ vs $1/z^4$ behavior, respectively).

V. SUMMARY AND CONCLUDING REMARKS

We studied numerically and analytically the propagation of waves in $\mathcal{PT}$-honeycomb photonic lattices, demonstrating the existence of conical diffraction arising solely from the presence of a spontaneous $\mathcal{PT}$-symmetry-breaking phase transition point. In spite of the fact that the eigenvectors are nonorthogonal and there is a collapse of the Hilbert space at the EP, the emerging cone is brighter and moves faster than the corresponding one of the passive structure. Although, the realization of such photonic structures is currently a challenging task, active electronic circuits, like the one proposed in Ref. [18], can be proven useful alternatives that might allow us to investigate experimentally wave propagation in extended $\mathcal{PT}$-symmetric lattices.

These findings raise several intriguing questions. For example, how does nonlinearity affect $\mathcal{PT}$-symmetric conical diffraction? What is the effect of disorder [37]? Is this behavior generic for any system at the spontaneously $\mathcal{PT}$-symmetry-breaking point? These intriguing questions are universal and relate to any field in which waves can propagate in a periodic potential. It is expected that in active metamaterials such phenomena will be present and they may have specific technological importance.

ACKNOWLEDGMENTS

T.K. and H.R. acknowledge support by a AFOSR No. FA 9550-10-1-0433 grant, NSF ECCS-1128571 grant and D.N.C. acknowledges a AFOSR No. FA 9550-10-1-0561 grant. V.K.'s work was supported via AFOSR LRIR 09RY04COR.

[1] M. V. Berry and M. R. Jeffrey, Prog. Opt. **50**, 13 (2007); M. V. Berry, M. R. Jeffrey, and J. G. Lunney, Proc. R. Soc. London A **462**, 1629 (2006).

[2] R. A. Indik and A. C. Newell, Opt. Express **14**, 10614 (2006).

[3] W. R. Hamilton, Trans. R. Irish Acad. **17**, 1 (1837).

[4] H. Lloyd, Trans. R. Irish Acad. **17**, 145 (1837).

[5] O. Peleg, G. Bartal, B. Freedman, O. Manela, M. Segev, and D. N. Christodoulides, Phys. Rev. Lett. **98**, 103901 (2007).

[6] O. Bahat-Treidel *et al.*, Opt. Lett. **33**, 2251 (2008).

[7] M. J. Ablowitz, S. D. Nixon, and Y. Zhu, Phys. Rev. A **79**, 053830 (2009); M. J. Ablowitz and Y. Zhu, *ibid.* **82**, 013840 (2010).

[8] R. I. Egorov *et al.*, Opt. Lett. **31**, 2048 (2006).

[9] O. Bahat-Treidel, O. Peleg, M. Grobman, N. Shapira, M. Segev, and T. Pereg-Barnea, Phys. Rev. Lett. **104**, 063901 (2010).

[10] A. Szameit, M. C. Rechtsman, O. Bahat-Treidel, and M. Segev,Phys. Rev. A **84**, 021806 (2011).

[11] K. G. Makris, R. El-Ganainy, D. N. Christodoulides, and Z. H. Musslimani, Phys. Rev. Lett. **100**, 103904 (2008).

[12] T. Kottos, Nat. Phys. **6**, 166 (2010).

[13] C. M. Bender and S. Boettcher, Phys. Rev. Lett. **80**, 5243 (1998); C. M. Bender, D. C. Brody, and H. F. Jones, *ibid.* **89**, 270401 (2002).

[14] M. Znojil, Phys. Lett. A **285**, 7 (2001); H. F. Jones, J. Phys. A **42**, 135303 (2009).

[15] C. M. Bender, Rep. Prog. Phys. **70**, 947 (2007); C. M. Bender, D. C. Brody, H. F. Jones, and B. K. Meister, Phys. Rev. Lett. **98**, 040403 (2007).

[16] C. E. Ruter *et al.*, Nat. Phys. **6**, 192 (2010).

[17] A. Guo, G. J. Salamo, D. Duchesne, R. Morandotti, M. Volatier-Ravat, V. Aimez, G. A. Siviloglou, and D. N. Christodoulides, Phys. Rev. Lett. **103**, 093902 (2009).

[18] J. Schindler, A. Li, M. C. Zheng, F. M. Ellis, and T. Kottos, Phys. Rev. A **84**, 040101(R) (2011).

[19] L. Feng, M. Ayache, J. Huang, Y.-L. Xu, M.-H. Lu, Y.-F. Chen, Y. Fainman, and A. Scherer, Science **333**, 729 (2011)

[20] M. C. Zheng, D. N. Christodoulides, R. Fleischmann, and T. Kottos, Phys. Rev. A **82**, 010103 (2010).

[21] E. M. Graefe and H. F. Jones, Phys. Rev. A **84**, 013818 (2011).

[22] S. Longhi, Phys. Rev. Lett. **103**, 123601 (2009).

[23] Z. Lin, H. Ramezani, T. Eichelkraut, T. Kottos, H. Cao, and D. N. Christodoulides, Phys. Rev. Lett. **106**, 213901 (2011).

[24] H. Ramezani, T. Kottos, R. El-Ganainy, and D. N. Christodoulides, Phys. Rev. A **82**, 043803 (2010).

[25] S. Longhi, Phys. Rev. A **82**, 031801 (2010); Y. D. Chong, L. Ge, and A. D. Stone, Phys. Rev. Lett. **106**, 093902 (2011).

[26] F. Nazari, M. Nazari, and M. K. Moravvej-Farshi, Opt. Lett. **36**, 4368 (2011).

[27] A. A. Sukhorukov, Z. Xu, and Y. S. Kivshar, Phys. Rev. A **82**, 043818 (2010).

[28] Z. H. Musslimani K. G. Makris, R. El-Ganainy, and D. N. Christodoulides, Phys. Rev. Lett. **100**, 030402 (2008).

[29] A. Mostafazadeh, J. Math. Phys. **43**, 205 (2002).

[30] A. Mostafazadeh, J. Math. Phys. **43**, 3944 (2002).

[31] A. Mostafazadeh, J. Phys. A **41**, 055304 (2008).

[32] C. M. Bender, M. V. Berry, and A. Mandilara, J. Phys. A **35**, L467 (2002).

[33] O. Bendix *et al.*, J. Phys. A **43**, 265305 (2010).

[34] Here we use the term "conical" diffraction in a rather loose fashion. Specifically, when the lattice is deformed, i.e., $t \neq 1$, the CD pattern becomes elliptic [6].

[35] K. Petermann, IEEE J. Quantum Electron. **15**, 566 (1979); A. E. Siegman, Phys. Rev. A **39**, 1264 (1989).

[36] M. V. Berry, J. Mod. Opt. **50**, 63 (2003); S.-Y. Lee, J. W. Ryu, J. B. Shim, S. B. Lee, S. W. Kim, and K. An, Phys. Rev. A **78**, 015805 (2008).

[37] O. Bendix, R. Fleischmann, T. Kottos, and B. Shapiro, Phys. Rev. Lett. **103**, 030402 (2009); C. T. West, T. Kottos, and T. Prosen, *ibid.* **104**, 054102 (2010).